Kinetic and Thermodynamic Studies of Iron(III) and Iron(IV) σ-Bonded Porphyrins. Formation and Reactivity of $[(OEP)Fe(R)]^{n+}$, Where OEP Is the Dianion of Octaethylporphyrin (n = 0, 1, 2, 3) and R = C_6H_5, 3,4,5-$C_6F_3H_2$, 2,4,6-$C_6F_3H_2$, C_6F_4H, or C_6F_5

Karl M. Kadish,*[,1a] Eric Van Caemelbecke,[1a] Elena Gueletii,[1a] Shunichi Fukuzumi,*[,1b] Kenichi Miyamoto,[1b] Tomoyoshi Suenobu,[1b] Alain Tabard,[1c] and Roger Guilard*[,1c]

Department of Chemistry, University of Houston, Houston, Texas 77204-5641, Department of Applied Chemistry, Faculty of Engineering, Osaka University, Suita, Osaka 565-0871, Japan, and LIMSAG, UMR 5633, Université de Bourgogne, Faculté des Sciences "Gabriel", 6 Boulevard Gabriel, 21000 Dijon, France

Received November 19, 1997

A series of high- and low-spin iron(III) phenyl and fluorophenyl octaethylporphyrin complexes are characterized by their electrochemical and spectroscopic properties in nonaqueous media. The investigated compounds are represented as (OEP)Fe(R), where R = C_6H_5, 3,4,5-$C_6F_3H_2$, 2,4,6-$C_6F_3H_2$, C_6F_4H, or C_6F_5 and OEP is the dianion of 2,3,7,8,12,13,17,18-octaethylporphyrin. The two $C_6F_3H_2$ complexes are of special interest in that these isomers differ in the spin state of the iron(III). Electrochemical studies indicate that three one-electron oxidations are seen for all of the (OEP)Fe(R) derivatives which were investigated both at room and low temperature under conditions where migration of the σ-bonded ligand does not occur on the time scale of the experiment. The first one-electron oxidation of each compound leads to an Fe(IV) porphyrin, and this is followed by a migration of the axial group from the iron center to one of the four nitrogen atoms independent of the nature of the axial group or the iron(III) spin state. The kinetics were examined to evaluate the migration rate constants in the presence and absence of pyridine as a sixth axial ligand. The results of this study show that the stronger the electron donor ability of the R group, the faster the migration rate in the case of the five-coordinate species. However, an increase in charge density at the metal center by axial coordination of pyridine retards the migration rate and this result is interpreted in terms of a rate determining electron transfer step from R to Fe(IV) of the singly oxidized species prior to the migration. Our results also show that the spin state of the iron(III) octaethylporphyrin is not a key factor which governs the migration of the axial ligand of the electrooxidized species. For the first time, an overall mechanism is proposed to explain the migration reaction in the σ-bonded iron porphyrin complexes.

Introduction

Organoiron derivatives have been identified as intermediates in several biological processes, including lipoxygenation catalyzed by lipoxygenase enzymes[2] and heme inactivation in hemoglobin, myoglobin, cytochrome P-450, and catalase.[3−7] These transient species are unstable and undergo a migration of the σ-bonded axial ligand from the heme iron to one of the four porphyrin ring nitrogens leading to the formation of *N*-substituted hemes.[8]

To understand the reactivity and role of these organoiron species in biological systems, a number of iron porphyrins possessing σ-bonded alkyl or aryl axial ligands have been synthesized and characterized over the last 15 years.[9−33] Our

(1) (a) University of Houston. (b) Osaka University. (c) Université de Bourgogne.
(2) Corey, E. J.; Wright, S. W.; Matsuda, S. P. T. *J. Am. Chem. Soc.* **1989**, *111*, 1452−1455.
(3) Ortiz de Montellano, P. R.; Kunze, K. L.; Augusto, O. *J. Am. Chem. Soc.* **1982**, *104*, 3545−3546.
(4) Ortiz de Montellano, P. R.; Kerr, D. E. *Biochemistry* **1985**, *24*, 1147−1152.
(5) Ortiz de Montellano, P. R.; Reich, N. O. In *Cytochrome P-450*; Ortiz de Montellano, P. R., Ed.; Plenum Press: New York, 1986; pp 273−314.
(6) Ortiz de Montellano, P. R. *Acc. Chem. Res.* **1987**, *20*, 289−294.
(7) Guilard, R.; Kadish, K. M. *Chem. Rev.* **1988**, *88*, 1121−1146.
(8) Lavallee, D. K. *The Chemistry and Biochemistry of N-Substituted Porphyrins*, 1st ed.; VCH Publishers: New York, 1987; p 313.
(9) Lexa, D.; Savéant, J.-M. *J. Am. Chem. Soc.* **1982**, *104*, 3503−3504.
(10) Ogoshi, H.; Sugimoto, H.; Yoshida, Z.-I.; Kobayashi, H.; Sakai, H.; Maeda, Y. *J. Organomet. Chem.* **1982**, *234*, 185−195.
(11) Mansuy, D.; Fontecave, M.; Battioni, J.-P. *J. Chem. Soc., Chem. Commun.* **1982**, 317−319.
(12) Mansuy, D.; Battioni, J.-P. *J. Chem. Soc., Chem. Commun.* **1982**, 638−639.
(13) Mansuy, D.; Battioni, J.-P.; Dupre, D.; Sartori, E. *J. Am. Chem. Soc.* **1982**, *104*, 6159−6161.
(14) Kunze, K. L.; Ortiz de Montellano, P. R. *J. Am. Chem. Soc.* **1983**, *105*, 1380−1381.
(15) Battioni, P.; Mahy, J.-P.; Gillet, G.; Mansuy, D. *J. Am. Chem. Soc.* **1983**, *105*, 1399−1401.
(16) Cocolios, P.; Lagrange, G.; Guilard, R. *J. Organomet. Chem.* **1983**, *253*, 65−79.
(17) Cocolios, P.; Laviron, E.; Guilard, R. *J. Organomet. Chem.* **1982**, *228*, C39−C42.
(18) Lançon, D.; Cocolios, P.; Guilard, R.; Kadish, K. M. *J. Am. Chem. Soc.* **1984**, *106*, 4472−4478.
(19) Lançon, D.; Cocolios, P.; Guilard, R.; Kadish, K. M. *Organometallics* **1984**, *3*, 1164−1170.
(20) Doppelt, P. *Inorg. Chem.* **1984**, *23*, 4009−4011.

S0020-1669(97)01470-5 CCC: $15.00
Published on Web 03/31/1998

own laboratories have concentrated, in large part, on the synthesis and characterization of σ-bonded iron porphyrins containing phenyl or perfluorophenyl groups of the type C_6H_5, C_6F_5, or C_6F_4H.[16−19,34−39] A migration of the σ-bonded axial ligand has been shown to occur upon the chemical or electrochemical oxidation of some synthetic σ-bonded iron(III) porphyrins,[3,7,13,22,34,36−38] but the exact conditions leading to the occurrence or absence of a migration reaction has yet to be completely understood.

The first electrochemical studies of (OEP)Fe(R) and (TPP)Fe(R)[18,40] showed that a migration of the σ-bonded R group was initiated by a one-electron oxidation but seemed to occur only for compounds containing a specific σ-bonded ligand and/or iron(III) spin state.[34,41] Electrogenerated $[(OEP)Fe(C_6H_5)]^+$ and $[(TPP)Fe(C_6H_5)]^+$ were shown to undergo an axial ligand migration, but this reaction was not observed on the cyclic voltammetry time scale for the same singly oxidized porphyrins containing σ-bonded C_6F_5 or C_6F_4H groups. This difference in reactivity between $[(P)Fe(C_6H_5)]^+$ and the perfluorophenyl derivatives, $[(P)Fe(C_6F_4H)]^+$ and $[(P)Fe(C_6F_5)]^+$, was first attributed to a difference in iron(III) spin state of the neutral compounds and/or a difference in the site of electron transfer of the singly oxidized species. The low-spin compounds containing C_6H_5 were proposed to be oxidized at the metal center, while the high-spin compounds containing C_6F_4H or C_6F_5 were proposed to be oxidized at the conjugated porphyrin π ring system. However, a more recent electrochemical study of (OETPP)Fe(C_6H_5), (OETPP)Fe(C_6F_5), and (OETPP)Fe(C_6F_4H)[39,40] indicates this analysis to be much too simplified since all three OETPP derivatives contain low-spin iron(III) and none of the $[(OETPP)Fe(R)]^+$ complexes undergoes a migration, despite the unequivocal formation of iron(IV) in singly oxidized $[(OETPP)Fe(C_6H_5)]^+$.[39] This result seems to clearly indicate that the iron(III) spin state is not a key factor governing the axial ligand migration of oxidized σ-bonded Fe(III) porphyrins.

Two additional results emerge from the electrochemical study of (OETPP)Fe(R).[39] The first is that doubly oxidized $[(OETPP)Fe^{IV}(C_6H_5)]^{2+}$ undergoes a slow migration reaction to give $[(N\text{-}C_6H_5OETPP)Fe^{III}]^{2+}$, and the second is that three well-defined one-electron oxidations are observed for the initial σ-bonded complex by cyclic voltammetry at high scan rates or low temperatures in benzonitrile containing 0.1 M tetrabutylammonium perchlorate (TBAP). The three oxidations are consistent with formation of an iron(IV) porphyrin followed by an iron(IV) porphyrin π cation radical and dication, and these latter two reactions at the porphyrin π ring system should also have been observed after the facile formation of $[(OEP)Fe^{IV}(C_6H_5)]^+$ and $[(TPP)Fe^{IV}(C_6H_5)]^+$ in benzonitrile containing 0.1 M TBAP.[18]

To explore this possibility, and to look for the expected third oxidation of other (P)Fe(R) derivatives, we have now systematically investigated the redox properties of five σ-bonded porphyrins in the OEP series under experimental conditions where a third oxidation might be observed at very positive potentials. We have also more closely examined the reactivity of the singly oxidized porphyrins on time scales longer than those of cyclic voltammetry and provide the first kinetic measurements for rate constants involving the conversion of $[(OEP)Fe(R)]^+$ to $[(N\text{-}ROEP)Fe]^+$.

The investigated porphyrins are represented as (OEP)Fe(R), where R = C_6H_5, 3,4,5-$C_6F_3H_2$, 2,4,6-$C_6F_3H_2$, C_6F_4H, or C_6F_5. The two (OEP)Fe($C_6F_3H_2$) isomers differ in the degree of steric hindrance between the axial ligand and the porphyrin macrocycle as well as in spin state of the Fe(III). The 3,4,5-$C_6F_3H_2$ derivative contains low-spin iron(III), and the 2,4,6-$C_6F_3H_2$ derivative contains high-spin iron(III) as shown in Chart 1.

Experimental Section

Chemicals. Benzonitrile (PhCN) was obtained from Aldrich Chemical Co. and distilled over P_2O_5 under vacuum prior to use. Absolute dichloromethane (CH_2Cl_2) over molecular sieves (Fluka Chemika) and anhydrous pyridine (Aldrich) were used without further purification. Tetra-*n*-butylammonium perchlorate (TBAP) was purchased from Sigma Chemical Co., recrystallized from ethyl alcohol, and dried under vacuum at 40 °C for at least 1 week prior to use. 2,3-Dichloro-5,6-dicyano-1,4-benzoquinone (DDQ) was obtained commercially and used without further treatment.

Synthesis of (OEP)Fe(R). The five investigated aryl σ-bonded iron porphyrins were prepared by reacting the corresponding aryl Grignard reagent with (OEP)FeCl according to literature procedures.[18,34] The synthesis of (OEP)Fe(R), where R = C_6H_5, C_6F_4H, or C_6F_5, has already been reported in the literature.[34] The (OEP)Fe(R) derivatives, where R = 3,4,5- and 2,4,6-$C_6F_3H_2$, have not previously been reported, and a description of their physicochemical properties is given below.

(OEP)Fe(3,4,5-$C_6F_3H_2$). UV−visible (CH_2Cl_2) λ_{max}, nm (10^{-3} ϵ, M^{-1} cm^{-1}): 390 (63), 531 (8), 554 (8). ^1H NMR (C_6D_6 from $SiMe_4$ at 300 K) δ, ppm: 8.14, −0.06 (16H, α-CH_2), −1.30 (24 H, β-CH_3), −77.90 (2 H, *o*-$H_{axial\ ligand}$), 5.84 (4 H, *meso*-H). ^{19}F NMR (using $CFCl_3$ as external reference at 294 K) δ, ppm: −120.8, −194.9 in C_5D_5N, −92.9, −206.5 in C_6D_6 ($F_{axial\ ligand}$). Mass spectrum (DEI): $M^{\bullet+}$, *m/z* 719 (66); $[M - C_6F_3H_2]^+$, *m/z* 588 (100). Anal. Calcd for $C_{42}H_{46}N_4F_3Fe$: C, 70.09; H, 6.44; N, 7.78. Found: C, 69.2; H, 6.7; N, 8.1.

(OEP)Fe(2,4,6-$C_6F_3H_2$). UV−vis (CH_2Cl_2) λ_{max}, nm (10^{-3} ϵ, M^{-1} cm^{-1}): 365 (58), 510(6), 537(6), 642(2). ^1H NMR (C_6D_6 from $SiMe_4$ at 300 K) δ, ppm: 38.9, 37.5 (16 H, α-CH_2), 5.5 (24 H, β-CH_3), −47.5

(21) Balch, A. L.; Renner, M. W. *Inorg. Chem.* **1986**, *25*, 303−307.
(22) Balch, A. L.; Renner, M. W. *J. Am. Chem. Soc.* **1986**, *108*, 2603−2608.
(23) Clarke, D. A.; Dolphin, D.; Grigg, R.; Johnson, A. W.; Pinnock, H. A. *J. Chem. Soc. C* **1968**, 881−885.
(24) Lexa, D.; Mispelter, J.; Savéant, J.-M. *J. Am. Chem. Soc.* **1981**, *103*, 6806−6812.
(25) Lexa, D.; Savéant, J.-M.; Battioni, J.-P.; Lange, M.; Mansuy, D. *Angew. Chem., Int. Ed. Engl.* **1981**, *20*, 578−579.
(26) Reed, C. A.; Mashiko, T.; Bentley, S. P.; Kastner, M. E.; Scheidt, W. R.; Spartalian, K.; Lang, G. *J. Am. Chem. Soc.* **1979**, *101*, 2948−2958.
(27) Balch, A. L.; Hart, R. L.; Latos-Grazynski, L.; Traylor, T. G. *J. Am. Chem. Soc.* **1990**, *112*, 7382−7388.
(28) Arasasingham, R. D.; Balch, A. L.; Hart, R. L.; Latos-Grazynski, L. *J. Am. Chem. Soc.* **1990**, *112*, 7566−7571.
(29) Arasasingham, R. D.; Balch, A. L.; Cornman, C. R.; Latos-Grazynski, L. *J. Am. Chem. Soc.* **1989**, *111*, 4357−4363.
(30) Arasasingham, R. D.; Balch, A. L.; Latos-Grazynski, L. *J. Am. Chem. Soc.* **1987**, *109*, 5846−5847.
(31) Li, Z.; Goff, H. M. *Inorg. Chem.* **1992**, *31*, 1547−1548.
(32) Shin, K.; Yu, B.-S.; Goff, H. M. *Inorg. Chem.* **1990**, *29*, 889−890.
(33) Arafa, I. M.; Shin, K.; Goff, H. M. *J. Am. Chem. Soc.* **1988**, *110*, 5228−5229.
(34) Guilard, R.; Boisselier-Cocolios, B.; Tabard, A.; Cocolios, P.; Simonet, B.; Kadish, K. M. *Inorg. Chem.* **1985**, *24*, 2509−2520.
(35) Kadish, K. M.; Tabard, A.; Lee, W.; Liu, Y. H.; Ratti, C.; Guilard, R. *Inorg. Chem.* **1991**, *30*, 1542−1549.
(36) Kadish, K. M.; D' Souza, F.; Van Caemelbecke, E.; Tabard, A.; Guilard, R. In *Proceedings of the Fifth International Symposium on Redox Mechanisms and Interfacial Properties of Molecules of Biological Importance*; Shultz, F. A., Taniguchi, I., Eds.; The Electrochemical Society, Inc.: Princeton, NJ, 1993; Vol. 93-II, pp 125−134.
(37) Kadish, K. M.; D'Souza, F.; Van Caemelbecke, E.; Villard, A.; Lee, J.-D.; Tabard, A.; Guilard, R. *Inorg. Chem.* **1993**, *32*, 4179−4185.
(38) Kadish, K. M.; Van Caemelbecke, E.; D'Souza, F.; Medforth, C. J.; Smith, K. M.; Tabard, A.; Guilard, R. *Organometallics* **1993**, *12*, 2411−2413.
(39) Kadish, K. M.; Van Caemelbecke, E.; D'Souza, F.; Medforth, C. J.; Smith, K. M.; Tabard, A.; Guilard, R. *Inorg. Chem.* **1995**, *34*, 2984−2989.
(40) Notation used: P, any porphyrin; OEP^{2-}, dianion of octaethylporphyrin; TPP^{2-}, dianion of tetraphenylporphyrin; $OETPP^{2-}$, dianion of octaethyltetraphenylporphyrin.
(41) Guilard, R.; Lecomte, C.; Kadish, K. M. *Struct. Bonding* **1987**, *64*, 205−268.

Chart 1

(OEP)Fe(3,4,5-$C_6F_3H_2$) S = 1/2 (OEP)Fe(2,4,6-$C_6F_3H_2$) S = 5/2

(4 H, *meso*-H). ^{19}F NMR (in C_5D_5N using $CFCl_3$ as external reference at 294 K) δ, ppm: −53.1, −82.8 ($F_{axial\ ligand}$). Mass spectrum (DEI): $M^{\bullet+}$, *m*/*z* 719 (28); $[M - C_6F_3H_2]^+$, *m*/*z* 588 (100). Anal. Calcd for $C_{42}H_{46}N_4F_3Fe$: C, 70.09; H, 6.44; N, 7.78. Found: C, 71.2; H, 6.9; N, 7.9.

Instrumentation. ^{1}H and ^{19}F NMR spectra were recorded at 500 MHz on a Bruker Avance DRX and at 200 MHz on a Bruker AC 200 spectrometers at the CSMUB ("Centre de Spectrométrie Moléculaire de l'Université de Bourgogne"). ESR spectra were recorded in toluene on a Bruker ESP 300 spectrometer equipped with an Oxford Instrument Cryostat. The *g* values were measured with respect to diphenylpicrylhydrazyl ($g = 2.0036 \pm 0.0003$). Electronic absorption spectra were recorded on a Varian Cary 5 spectrophotometer. Mass spectra were obtained with a Kratos Concept 32S spectrometer, and the data were collected and processed using a Sun 3/80 workstation.

Cyclic voltammetry was carried out with an an EG&G Princeton Applied Research model 173 Potentiostat/Galvanostat coupled with an EG&G PARC model 175 Universal Progammer. Current−voltage curves were recorded on an EG&G Princeton Applied Research model RE-0151 *X*−*Y* recorder. A three-electrode system was used and consisted of a glassy carbon button or a platinum working electrode, a platinum wire counter electrode, and a saturated calomel reference electrode (SCE). The reference electrode was separated from the bulk of the solution by a fritted-glass bridge filled with the solvent/supporting electrolyte mixture. All potentials are referenced to the SCE.

Spectroelectrochemical experiments were performed at a platinum thin-layer electrode whose design is described in the literature.[42] The potentials were applied and monitored with an EG&G Princeton Applied Research model 173 potentiostat. Time-resolved UV−visible spectra were recorded with a Hewlett-Packard model 8453 diode array spectrophotometer.

Kinetic Measurements. The chemical oxidation of (OEP)Fe(R) (R = C_6H_5, 3,4,5-$C_6F_3H_2$, 2,4,6-$C_6F_3H_2$, C_6F_4H) was accomplished by adding an aliquot (50 μL) of DDQ (3.0×10^{-2} M) in CH_2Cl_2 to a quartz cuvette (10 mm i.d.) which contained (OEP)Fe(R) (1.2×10^{-4} M) and TBAP (0.2 M) in deaerated CH_2Cl_2 (3.0 mL). The UV−visible spectral changes associated with the initial electron transfer from (OEP)Fe(R) to DDQ and the subsequent migration of the σ-bonded ligand from the singly oxidized porphyrin were monitored in the dark at 298 K using a Hewlett-Packard model 8452A or 8453 diode array spectrophotometer. Similar experiments were carried out in the case of (OEP)Fe(R)(py).

Theoretical Calculations. The HOMO energy level calculations of phenyl and perfluorophenyl anions, i.e., $C_6H_5^-$, 3,4,5-$C_6F_3H_2^-$, 2,4,6-$C_6F_3H_2^-$, 2,3,5,6-$C_6F_4H^-$, and $C_6F_5^-$, were performed using the MOPAC program (Ver. 6) which is incorporated in the MOLMOLIS program by Daikin Industries, Ltd. The PM3 Hamiltonian was used for the semiempirical MO calculations.[43] Final geometries and energetics were obtained by optimizing the total molecular energy with respect to all structural variables.

Results and Discussion

Spectroscopic Characterization of (OEP)Fe(R). The five investigated (OEP)Fe(R) derivatives vary in the nature of the axial ligand, with the number and positions of the fluorine atoms on the R group determining the spin state of the initial Fe(III) complex. The spin state of iron(III) porphyrins is known to depend on the ligand field strength of the fifth or sixth axial ligand,[44] and a conversion from low-spin Fe(III) to high-spin Fe(III) is observed upon going from (OEP)Fe(C_6H_5) to either one of the two perfluorophenylporphyrins, (OEP)Fe(C_6F_5) or (OEP)Fe(C_6F_4H).[34]

A change in the position of the fluorine atoms from the meta to the ortho positions of the σ-bonded aryl group on (OEP)Fe($C_6F_3H_2$) will also induce a change in the iron(III) spin state as indicated by ^{1}H NMR spectra. (OEP)Fe(3,4,5-$C_6F_3H_2$) is in a low-spin state ($S = {}^1/_2$). In contrast, (OEP)Fe(2,4,6-$C_6F_3H_2$) contains high-spin Fe(III) ($S = {}^5/_2$) and exhibits two typical ESR signals at $g = 5.85$ and 2.06 in toluene at 4 K. However, as expected, the two compounds are in a low-spin state when a pyridine ligand is six-coordinated to the iron center. This is unambiguously shown by the ^{19}F NMR chemical shifts in C_5D_5N.[35]

The room-temperature UV−visible spectra of (OEP)Fe(R) support the NMR-based assignments of spin state in the case of the two $C_6F_3H_2$ derivatives. The spectrum of low-spin (OEP)Fe(3,4,5-$C_6F_3H_2$) is similar to that of low-spin (OEP)Fe(C_6H_5),[16] while the spectrum of high-spin (OEP)Fe(2,4,6-$C_6F_3H_2$) is comparable to that of high-spin (OEP)Fe(C_6F_4H)[34] (see Table 1). The differences in electronic properties between the axial ligands of (OEP)Fe(3,4,5-$C_6F_3H_2$) and (OEP)Fe(2,4,6-$C_6F_3H_2$) are smaller than the differences in electronic properties between the axial ligands of (OEP)Fe(C_6H_5) and (OEP)Fe(C_6F_5).[45,46] Thus, the fact that two different spin states are seen for (OEP)Fe(3,4,5-$C_6F_3H_2$) and (OEP)Fe(2,4,6-$C_6F_3H_2$) indicates that the iron spin state in the (OEP)Fe(R) is quite dependent on the nature of the axial ligands.

Electrochemistry of (OEP)Fe(R) in CH_2Cl_2. Figure 1 illustrates cyclic voltammograms for oxidation and reduction of the five (OEP)Fe(R) derivatives in CH_2Cl_2 containing 0.2 M TBAP at −50 °C. Each σ-bonded porphyrin undergoes one reversible reduction and three reversible oxidations at potentials between $E_{1/2} = -0.86$ and +1.83V vs SCE. Two of the compounds (R = C_6F_4H, C_6F_5) also show a second irreversible reduction at $E_{pc} \approx -1.80$V. Previous electrochemical studies of (OEP)Fe(R) were carried out only in PhCN at room temperature, and the first one-electron reduction was invariably accompanied by a loss of the σ-bonded ligand under these experimental conditions.[34] The low-temperature cyclic voltammograms in Figure 1 therefore provide the first reversible $E_{1/2}$ values for reduction of an (OEP)Fe(R) complex with C_6F_4H and C_6F_5 axial ligands.

The most significant feature of Figure 1 is that all five σ-bonded porphyrins undergo three one-electron oxidations, and this can only be accounted for by one of the three reactions being assigned to an Fe(III)/Fe(IV) transition and the other two to an oxidation of the conjugated porphyrin macrocycle. As will be demonstrated in the following sections, the first one-electron oxidation of (OEP)Fe(R) invariably results in the formation of an Fe(IV) complex while the latter two reactions are proposed to involve an electron abstraction from the porphyrin π ring system.

The half-wave potentials for each process in Figure 1 are summarized in Table 2 under different experimental conditions,

(42) Lin, X. Q.; Kadish, K. M. *Anal. Chem.* **1985**, *57*, 1498−1501.
(43) Stewart, J. J. P. *J. Comput. Chem.* **1989**, *10*, 209−221.
(44) (a) Scheidt, W. R.; Lee, Y. J. *Struct. Bonding* **1987**, *64*, 1−70. (b) Palmer, G. In *Iron Porphyrins*; Lever, A. B. P., Gray, H. B., Eds.; Addison-Wesley: Reading, MA, 1983; Vol. II, pp 43−88.
(45) Adcock, W.; Khor, T.-C. *J. Am. Chem. Soc.* **1978**, *100*, 7799−7810.
(46) Hansch, C.; Leo, A.; Taft, R. W. *Chem. Rev.* **1991**, *91*, 165−195.

Table 1. UV−Visible Data of (OEP)Fe(R) and $[(OEP)Fe(R)]^+$ in CH_2Cl_2, 0.2 M TBAP

			λ_{max}, nm ($\epsilon \times 10^{-3}$, M^{-1} cm^{-1})				
			Soret bands		visible bands		
compound	R	spin state[a]					
(OEP)Fe(R)	C_6H_5	ls		391 (62)	521 (6)	552 (7)	
	3,4,5-$C_6F_3H_2$	ls		390 (63)	531 (8)	554 (8)	
	2,4,6-$C_6F_3H_2$	hs	365 (58)		510 (6)	537 (6)	642 (2)
	C_6F_4H	hs	367 (63)		510 (6)	536 (5)	646 (2)
$[(OEP)Fe(R)]^+$	C_6H_5[b]	*c*		389 (57)	498 (sh)	525 (7)	−
	3,4,5-$C_6F_3H_2$	*c*		391 (49)	499 (sh)	531 (13)	626 (0.6)
	2,4,6-$C_6F_3H_2$	*c*	374 (59)		500 (sh)	535 (23)	641 (0.4)
	C_6F_4H	*c*	374 (59)		500 (sh)	531 (18)	641 (0.4)

[a] Assignment of spin state based on NMR spectra (ls, low spin; hs, high spin) at room temperature. [b] Spectrum of unstable product obtained after 10 s of electrolysis. [c] Spin state has not been assigned.

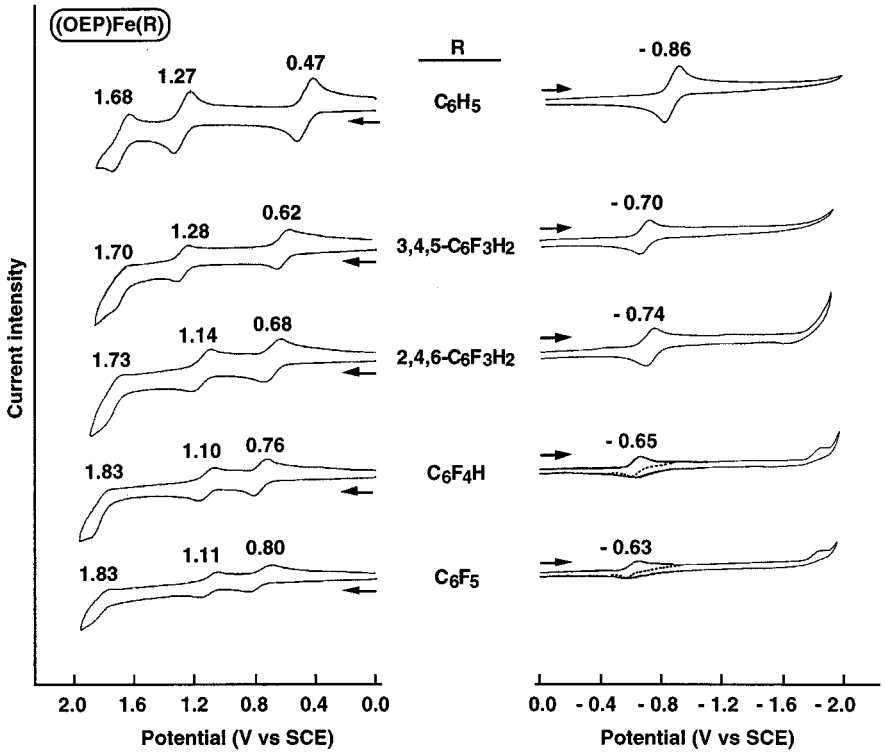

Figure 1. Low-temperature (−50 °C) cyclic voltammograms of (OEP)Fe(R) derivatives in CH_2Cl_2 containing 0.2 M TBAP.

and the four electrode reactions are proposed to occur as shown in eqs 1−4. The given iron oxidation state assignments are

$$(OEP)Fe^{III}(R) \rightleftarrows [(OEP)Fe^{IV}(R)]^+ + e^- \quad (1)$$

$$[(OEP)Fe^{IV}(R)]^+ \rightleftarrows [(OEP)Fe^{IV}(R)]^{2+} + e^- \quad (2)$$

$$[(OEP)Fe^{IV}(R)]^{2+} \rightleftarrows [(OEP)Fe^{IV}(R)]^{3+} + e^- \quad (3)$$

$$(OEP)Fe^{III}(R) + e^- \rightleftarrows [(OEP)Fe^{II}(R)]^- \quad (4)$$

consistent with previous analysis of the (OEP)Fe(C_6H_5) electrode reactions[18] and differ only by the presence of a third oxidation (Reaction 3) which is not observable in PhCN due to the more limited anodic potential range of this solvent. The potentials for the first reduction of (OEP)Fe(R) (Reaction 4) vary from $E_{1/2} = -0.86$ V for (OEP)Fe(C_6H_5) to -0.63 V for (OEP)-Fe(C_6F_5) and a similar positive shift is seen upon going from the first oxidation of (OEP)Fe(C_6H_5) ($E_{1/2} = +0.47$ V) to the first oxidation of (OEP)Fe(C_6F_5) ($E_{1/2} = +0.80$ V). These data indicate that both the first oxidation and the first reduction of (OEP)Fe(R) are strongly dependent upon the number and the position of the fluorine atoms on the axial ligand, and this is consistent with the metal-centered electron-transfer reactions shown in eqs 1 and 4. However, it is important to note that the relationship between $E_{1/2}$ and electron donor properties of the σ-bonded axial ligand do not follow a simple relationship with the number of F atoms, independent of Fe(III) spin state, as was previously suggested.[39] This is discussed in later sections of the manuscript.

UV−Visible Characterization of $[(OEP)Fe(R)]^+$. Metal-centered electrode reactions of metalloporphyrins are generally accompanied by only small changes in the porphyrin Soret band, while ring-centered reactions are often characterized by a large decrease in the Soret band intensity due to loss of the ring conjugation.[47] The best examples in the case of σ-bonded porphyrins are given by the conversion of (OETPP)M(C_6H_5) to $[(OETPP)M(C_6H_5)]^+$ where M = Fe or In in PhCN.[39] The one-electron oxidation of (OETPP)Fe(C_6H_5) involves an Fe(III)/

(47) Felton, R. H. In *The Porphyrins*; Dolphin, D., Ed.; Academic: New York, 1978; Vol. V, pp 53−125.

Table 2. Half-Wave Potentials (V vs SCE) for Oxidation and Reduction of (OEP)Fe(R) in Solvents Containing 0.2 M TBAP

electrode reaction	axial ligand, R	initial Fe(III) spin state (RT)	−50 °C		room temperature	
			CH_2Cl_2	CH_2Cl_2/pyr[a]	CH_2Cl_2	PhCN
1st oxidation	C_6H_5	ls	0.47	0.31	0.45	0.48[b]
	3,4,5-$C_6F_3H_2$	ls	0.62	0.49	0.64	0.66
	2,4,6-$C_6F_3H_2$	hs	0.68	0.57	0.73	0.76
	C_6F_4H	hs	0.76	0.73	0.81	0.79[c]
	C_6F_5	hs	0.80		−	0.87[c]
2nd oxidation	C_6H_5	ls	1.27		−	1.30[b]
	3,4,5-$C_6F_3H_2$	ls	1.28		1.31	1.31
	2,4,6-$C_6F_3H_2$	hs	1.14		1.23	1.19
	C_6F_4H	hs	1.10		1.22	1.14[c]
	C_6F_5	hs	1.11		−	1.18[c]
3rd oxidation	C_6H_5	ls	1.68		−	−
	3,4,5-$C_6F_3H_2$	ls	1.70		−	−
	2,4,6-$C_6F_3H_2$	hs	1.73		−	−
	C_6F_4H	hs	1.83		−	−
	C_6F_5	hs	1.83		−	−
1st reduction	C_6H_5	ls	−0.86			
	3,4,5-$C_6F_3H_2$	ls	−0.70			
	2,4,6-$C_6F_3H_2$	hs	−0.74			
	C_6F_4H	hs	−0.65			
	C_6F_5	hs	−0.63			

[a] [py] = 0.12 M. [b] Data from: Lançon, D.; Cocolios, P.; Guilard, R.; Kadish, K. M. *J. Am. Chem. Soc.* **1984**, *106*, 4472−4478. [c] Data from: Guilard, R.; Boisselier−Cocolios, B.; Tabard, A.; Cocolios, P.; Simonet, B.; Kadish, K. M. *Inorg. Chem.* **1985**, *24*, 2509−2520.

Fe(IV) reaction, and, as expected, the singly oxidized iron porphyrin shows only a 9 nm shift in the position of the Soret band and no loss in Soret band intensity. This contrasts with the oxidation of (OETPP)In(C_6H_5) where a porphyrin π cation radical is generated, leading to a UV−visible spectrum whose Soret band has virtually disappeared.[39]

The UV−visible spectra of singly oxidized $[(OEP)Fe(R)]^+$ also provide strong indirect evidence for the site of electron abstraction. The spectral data for each neutral and singly oxidized porphyrin are summarized in Table 1. As seen in this table, only relatively small changes occur upon going from (OEP)Fe(R) to $[(OEP)Fe(R)]^+$ independent of the initial Fe(III) spin state or the number of F atoms on the σ-bonded axial ligand. For example, the two low-spin derivatives, (OEP)Fe(C_6H_5) and (OEP)Fe(3,4,5-$C_6F_3H_2$), have a Soret band close to 390 nm both in their neutral and singly oxidized states. The two high-spin porphyrins have a Soret band at around 366 nm in the neutral state and 374 nm in the singly oxidized state. Most importantly, the spectral features of $[(OEP)Fe(R)]^+$ are almost identical for all of the singly oxidized compounds (Table 1), and this can only be interpreted in terms of the same metal oxidation state assignment, i.e., Fe^{IV} in $[(OEP)Fe(R)]^+$.

The spectroscopic data discussed above indicate that all five investigated (OEP)Fe(R) derivatives are oxidized at the metal center to generate Fe(IV) as previously shown for (OEP)Fe(C_6H_5).[18] The reversible half-wave potentials for these metal-centered reactions are fairly insensitive to the nature of the solvent (PhCN or CH_2Cl_2) or solution temperature between 25 and −50 °C in CH_2Cl_2 (see Table 2), but they do depend strongly on the nature of the axial ligand of the initial Fe(III) complex. This is not the case for electrode reactions involving the conjugated porphyrin macrocycle. Indeed, the second oxidation (Figure 2) and third oxidation of (OEP)Fe(R), as well as the first oxidation of (OEP)In(R) and (OEP)Tl(R) (R = C_6H_5, C_6F_4H, C_6F_5),[48,49] all involve the porphyrin π ring system but have $E_{1/2}$ values which do not vary significantly with the nature of the axial ligand.

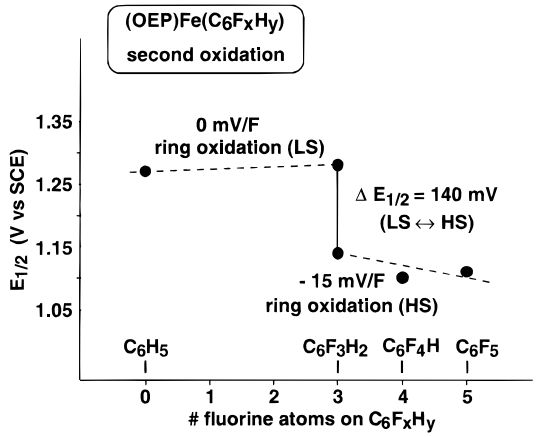

Figure 2. Relationship between $E_{1/2}$ for the second oxidation of (OEP)Fe($C_6F_xH_y$) and the number of fluorine atoms on the axial ligand.

In the first electrochemical study of (OEP)Fe(R),[34] it was pointed out that an overall 390 mV difference in half-wave potentials is observed between the same oxidations or reductions of (OEP)Fe(C_6H_5) and (OEP)Fe(C_6F_5) in PhCN. The perfluorophenyl species were harder to oxidize and easier to reduce by approximately 80 mV per added electron-withdrawing F group upon going from (OEP)Fe(C_6H_5) to (OEP)Fe(C_6F_5), and this was attributed to a purely inductive effect of the σ-bonded axial ligand. A similar potential difference is observed in CH_2Cl_2 at room temperature, but smaller values of 330 mV (oxidation) or 230 mV (reduction) are seen in CH_2Cl_2 at low temperature. However, an analysis of the data for all five compounds clearly shows that only a part of the difference between $E_{1/2}$ for reduction of (OEP)Fe(C_6H_5) and (OEP)Fe(C_6F_5) is due to the inductive effect of the F groups with the remainder being due to the specific high- or low-spin state of the Fe(III) ion in (OEP)Fe(R).

The key compounds which lead to this conclusion are (OEP)Fe(3,4,5-$C_6F_3H_2$), which is low spin, and (OEP)Fe(2,4,6-$C_6F_3H_2$), which is high spin. As seen in Table 2 and Figure 3, high-spin (OEP)Fe(2,4,6-$C_6F_3H_2$) is both harder to oxidize and harder to reduce (by 60−100 mV) than the low-spin (OEP)Fe(3,4,5-$C_6F_3H_2$) derivative. This difference cannot be simply

(48) Kadish, K. M.; Boisselier-Cocolios, B.; Cocolios, P.; Guilard, R. *Inorg. Chem.* **1985**, *24*, 2139−2147.
(49) Kadish, K. M.; Tabard, A.; Zrineh, A.; Ferhat, M.; Guilard, R. *Inorg. Chem.* **1987**, *26*, 2459−2466.

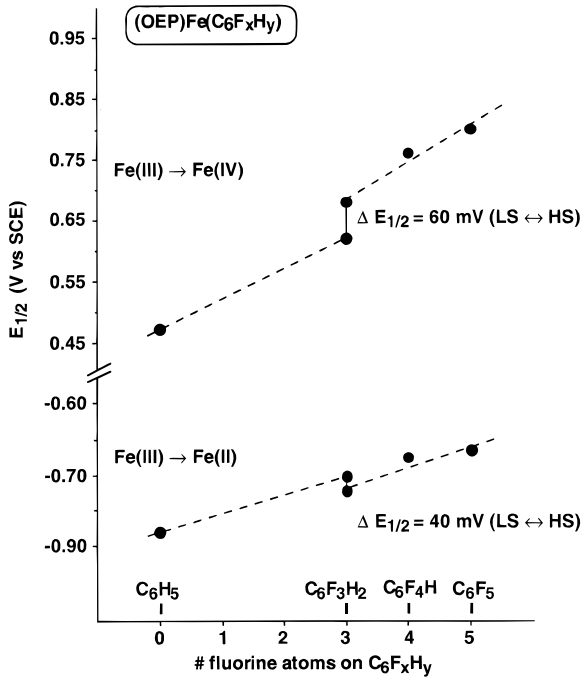

Figure 3. Dependence of $E_{1/2}$ for first oxidation and first reduction of (OEP)Fe($C_6F_xH_y$) on the number of fluorine atoms of the σ-bonded axial ligand.

related to a difference in inductive effects of the fluorine atoms between the two compounds since a purely inductive effect would shift the half-wave potentials for oxidation and reduction in the same direction, *which is clearly not the case*.

Kinetics and Mechanism of R Group Migration from [(OEP)Fe(R)]$^+$. The first published reports of phenyl group migration from electrogenerated [(TPP)Fe(C_6H_5)]$^+$ or [(OEP)-Fe(C_6H_5)]$^+$ related this reaction to the presence of an Fe(IV) oxidation state which was initially postulated on the basis of UV−visible and electrochemical data[19] and later proven on the basis of NMR spectra for several singly oxidized σ-bonded derivatives.[22] At the same time, the stability of [(P)Fe(C_6F_5)]$^+$- and [(P)Fe(C_6F_4H)]$^+$ was explained[34] in terms of a different site of electron transfer, i.e., the formation of an Fe(III) porphyrin π cation radical in the singly oxidized species. More extensive results, now described in this present paper, clearly point to the generation of an Fe(IV) oxidation state in all of the investigated [(OEP)Fe(R)]$^+$ derivatives, independent of iron spin state, and this leads to the conclusion that a migration reaction might actually occur for [(P)Fe(C_6F_5)]$^+$ and [(P)Fe(C_6F_4H)]$^+$ on longer time scales than those previously studied.

To investigate this possibility, we measured the rate constant for migration of C_6H_5 in [(OEP)Fe(C_6H_5)]$^+$ and also monitored the much slower time-dependent changes in UV−visible spectra of the other [(OEP)Fe(R)]$^+$ complexes after the chemical or electrochemical oxidation of (OEP)Fe(R). Of special importance was an investigation of the two [(OEP)Fe($C_6F_3H_2$)]$^+$ complexes since the 3,4,5-$C_6F_3H_2$ derivative contains low-spin Fe(III) and the 2,4,6-$C_6F_3H_2$ species contains high-spin Fe(III). Surprisingly, both $C_6F_3H_2$ complexes, as well as [(OEP)Fe-(C_6F_4H)]$^+$, undergo a metal-to-nitrogen migration of the σ-bonded axial ligand, and the resulting spectral data in the case of [(OEP)Fe(3,4,5-$C_6F_3H_2$)]$^+$ is shown in Figure 4.

The axial ligand migration rates for [(OEP)Fe(R)]$^+$ were determined by monitoring the time-dependent spectral changes as [(*N*-ROEP)Fe]$^+$ is formed after the one-electron oxidation of (OEP)Fe(R) in CH_2Cl_2 containing 0.2 M TBAP. In the case

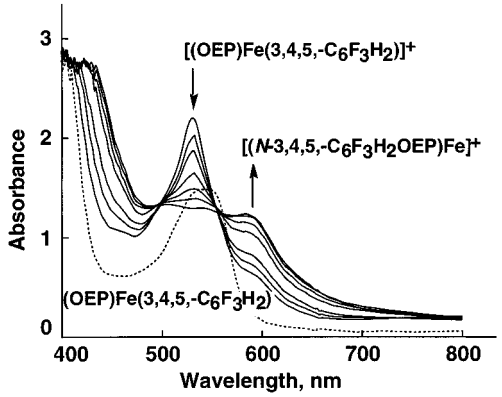

Figure 4. UV−visible spectral changes observed upon addition of 5.0 $\times$ 10^{-4} M DDQ to a CH_2Cl_2 solution containing (OEP)Fe(3,4,5-$C_6F_3H_2$) (1.2 $\times$ 10^{-4} M) and 0.2 M TBAP at 298K; t = 0, 60, 135, 325, 520, 840, and 2930 s.

Table 3. Rate Constants for R Group Migration of [(OEP)Fe(R)]$^+$ and [(OEP)Fe(R)(py)]$^+$ in CH_2Cl_2 Containing 0.2 M TBAP at 298 K

axial ligand, R		k_{mig}, s^{-1} [a]	
group	I_p [b]	[(OEP)Fe(R)]$^+$	[(OEP)Fe(R)(py)]$^+$ [c]
C_6H_5	2.06	2.8 $\times$ 10^{-2}	1.2 $\times$ 10^{-3}
3,4,5-$C_6F_3H_2$	2.97	4.6 $\times$ 10^{-3}	5.9 $\times$ 10^{-4}
2,4,6-$C_6F_3H_2$	3.35	1.7 $\times$ 10^{-4}	no migration
C_6F_4H	3.68	1.3 $\times$ 10^{-4}	no migration

[a] Rate constants good to ±5%. [b] The ionization potentials, I_p, were calculated by using the PM3 method. [c] Measured in CH_2Cl_2 containing 0.2 M TBAP and 0.12 M pyridine.

of (OEP)Fe(3,4,5-$C_6F_3H_2$), the migration rate constant was determined by simultaneously monitoring a decay in the peak at 531 nm and the rise of a new band at ca. 586 nm (see Figure 4). The migration rate obeys first-order kinetics, and this is also the case for the other three singly oxidized porphyrins whose migration rate constants (k_{mig}) at 298 K are summarized in Table 3. As seen in this table, the k_{mig} values vary by 2 orders of magnitude among the four investigated Fe(IV) complexes in CH_2Cl_2 and increase with increasing electron donor ability of the R group. For example, k_{mig} = 1.3 $\times$ 10^{-4} s^{-1} for [(OEP)-Fe(C_6F_4H)]$^+$ and 2.8 $\times$ 10^{-2} s^{-1} for [(OEP)Fe(C_6H_5)]$^+$ in CH_2Cl_2. The migration rate constants and half-wave potentials are both dependent on the donor properties of the σ-bonded axial ligand, and a good correlation therefore exists between these values and the ionization potential of the anionic axial ligand. This correlation is shown in Figure 5.

The effect of pyridine on the migration rate constant was also examined in the present paper since earlier studies of (OEP)-Fe(C_6H_5)(py) had indicated a stabilization of the oxidized complex by pyridine and a slowing down of the migration rate in PhCN/py mixtures.[19] No other (OEP)Fe(R)(py) complexes have since been investigated as to a migration reaction after electrooxidation, and the known[35] spin state conversion upon going from S = $^5/_2$, (OEP)Fe(C_6F_4H) to S = $^1/_2$, (OEP)Fe-(C_6F_4H)(py) was therefore of interest in terms of relating the iron(III) spin state in (OEP)Fe(R)(py) to the presence or absence of a migration reaction in the electrooxidized species.

The eight compounds which were kinetically investigated are represented by (OEP)Fe(R) and (OEP)Fe(R)(py), where R = C_6H_5, 3,4,5-$C_6F_3H_2$, 2,4,6-$C_6F_3H_2$, and C_6F_4H, and the resulting kinetic data are listed in Table 3. The k_{mig} decreases by 2 orders of magnitude upon going from [(OEP)Fe(C_6H_5)]$^+$ to [(OEP)-Fe(C_6F_4H)]$^+$, by about 1 order of magnitude upon going from [(OEP)Fe(C_6H_5)]$^+$ to [(OEP)Fe(C_6H_5)(py)]$^+$, and by a factor

Scheme 1

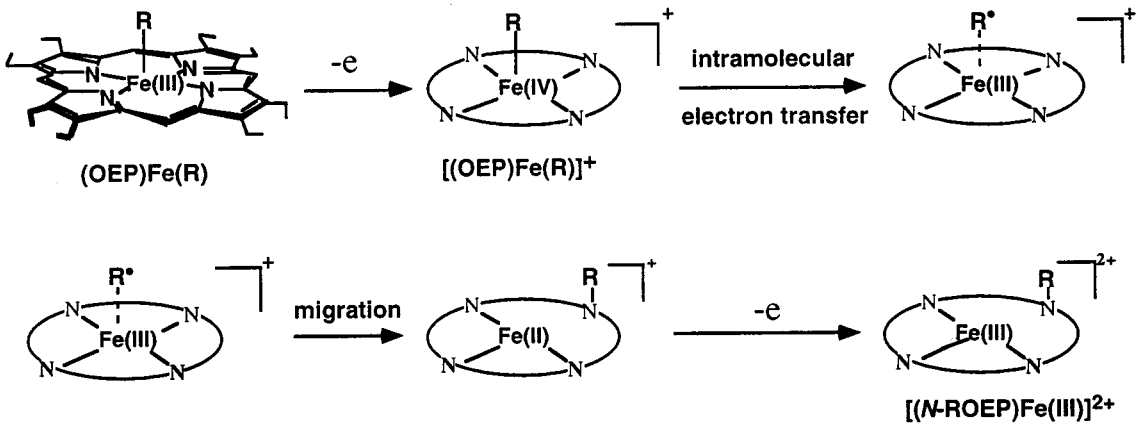

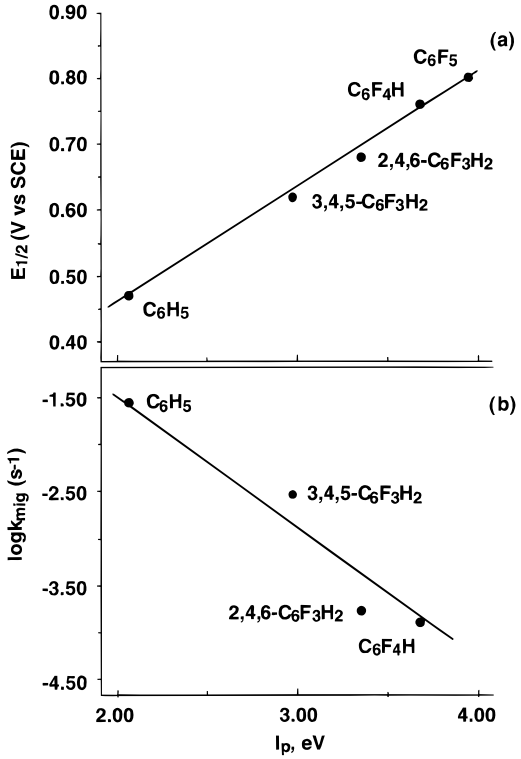

Figure 5. Relationships between (a) $E_{1/2}$ for oxidation of (OEP)Fe($C_6F_xH_y$) and (b) the axial ligand migration rate constant and the calculated ionization potential of the phenyl and perfluorophenyl anions (see Experimental Section for calculation of I_p).

of 2 upon going from [(OEP)Fe(C_6H_5)(py)]$^+$ to [(OEP)Fe(3,4,5-$C_6F_3H_2$)(py)]$^+$. No migration reaction at all can be detected in the case of [(OEP)Fe(2,4,6-$C_6F_3H_2$)(py)]$^+$ or [(OEP)Fe(C_6F_4H)(py)]$^+$, the two compounds which have the weakest electron-donating σ-bonded R groups. It is especially important to note that both low-spin six-coordinated compounds contain high-spin iron(III) prior to coordination with pyridine. The relevant ligand-binding reaction of the neutral and singly oxidized porphyrins are shown in eqs 5 and 6, and a summary of the log K values as determined in CH_2Cl_2 is given in Table 4.

$$(OEP)Fe^{III}(R) + py \rightleftarrows (OEP)Fe^{III}(R)(py) \quad (5)$$

$$[(OEP)Fe^{IV}(R)]^+ + py \rightleftarrows [(OEP)Fe^{IV}(R)(py)]^+ \quad (6)$$

An increased electron donation from the σ-bonded R group to the iron center of (OEP)Fe(R) will result in a negative shift

Table 4. Pyridine Binding Constants (K_f) for Neutral and Singly Oxidized (OEP)Fe(R) Complexes in CH_2Cl_2

	log K_f	
axial ligand, R	(OEP)Fe(R)(py)	[(OEP)Fe(R)(py)]$^+$
C_6H_5	1.9	3.7
3,4,5-$C_6F_3H_2$	2.6	4.2
2,4,6-$C_6F_3H_2$	1.4	4.1
C_6F_4H	1.5	4.5

of the $E_{1/2}$ values for oxidation, and a similar shift in $E_{1/2}$ is observed upon coordination of pyridine to form (OEP)Fe(R)(py) (see Table 2). This shift in potential is due to an increase in charge density on the iron center of the neutral complex from which the electron is removed. However, once the oxidation has occurred and [(OEP)Fe^{IV}(R)]$^+$ is generated, an increase in the donor ability of the R group will accelerate the migration rate while an increased electron donation from the pyridine axial ligand to the iron(IV) center will decelerate the migration rate (see Table 3). Such an opposite effect on the migration rate constants suggests a rate-determining intramolecular electron transfer from R to Fe(IV) as a first step in the metal to nitrogen migration of [(OEP)Fe(R)]$^+$. This is shown in Scheme 1.

The stronger the electron donor ability of R, the faster is the intramolecular electron transfer from R to Fe(IV). In contrast, the intramolecular electron transfer from the axial ligand, R, to the Fe(IV) center of (OEP)Fe(R)(py) is slowed upon coordination of pyridine which will increase the charge density at the Fe(IV) center. The effect of pyridine coordination is largest for the σ-bonded complex with the strongest electron-withdrawing σ-bonded axial ligand, i.e., for (OEP)Fe(C_6F_4H), a compound which undergoes a slow migration in CH_2Cl_2 but not in CH_2Cl_2/pyridine mixtures where [(OEP)Fe(C_6F_4H)(py)]$^+$ appears to be stable.

Evidence for the Formation of Fe(II) in Singly Reduced (OEP)Fe(R). Evidence for formation of Fe(II) after the first one electron reduction of (OEP)Fe(R) is based largely on the electrochemical data which differs substantially from that of other (OEP)M(R) complexes, with M = Al, In, Ga, or Tl, which are known to undergo reduction at the conjugated macrocycle to give porphyrin π anion radicals. These differences are best shown by examining the dependence of $E_{1/2}$ for the first reduction of (OEP)M(R) on both the electronegativity of the central metal ion and the donor properties of the axial ligand. This comparison is illustrated in Figure 6a which shows that the first reduction of (OEP)M(C_6H_5) is virtually independent of the central metal ion when M = Al, In, Ga, or Tl. These four main group complexes are all reduced to π anion radicals at half-wave potentials of -1.40 to -1.44 V vs SCE as

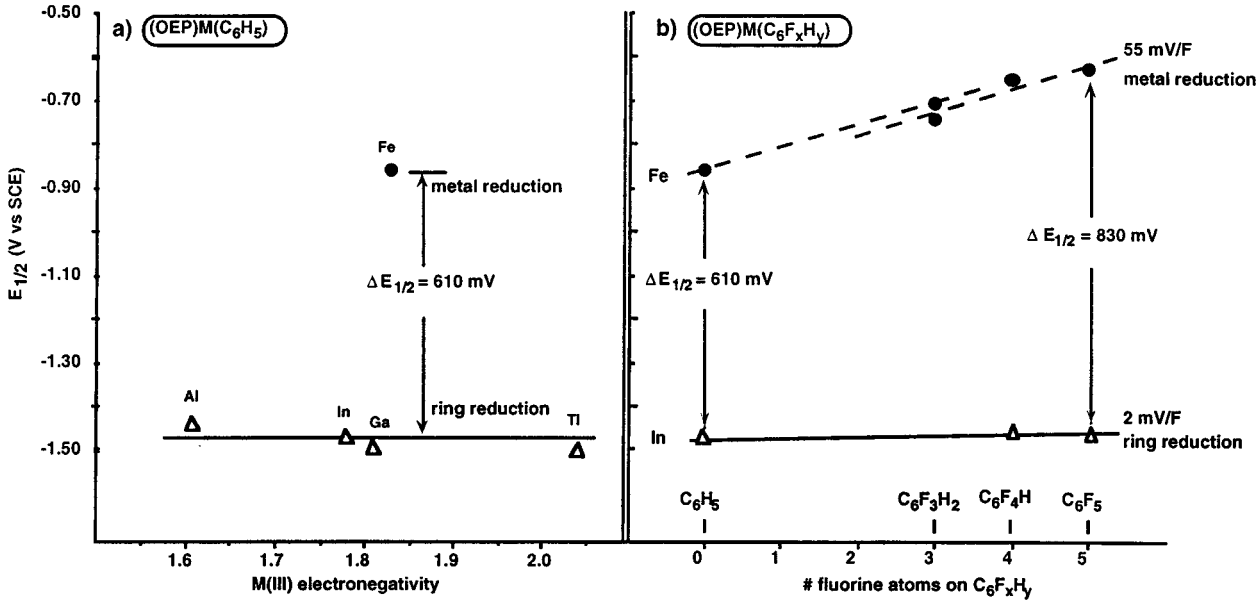

Figure 6. Dependence of the first reduction potential (a) of (OEP)M(C_6H_5) on the central metal electronegativity of the complex, where M = Fe, Al, Ga, In, or Tl, and (b) of (OEP)M($C_6F_xH_y$) on the number of fluorine atoms of the axial ligand for complexes where M = Fe or In and $x + y = 5$.

compared to the first reduction of (OEP)Fe(C_6H_5) which is reduced at the central metal ion and has an $E_{1/2}$ of −0.86 V under the same experimental conditions even though the Fe(III) electronegativity is similar to that of Ga(III).

The reductions of (OEP)M(R) are also virtually independent of the axial ligand when this electrode reaction occurs at the conjugated macrocycle as is the case for the main group complexes. For example, the (OEP)In(R) derivatives show only a 2 mV shift in potentials between $E_{1/2}$ for the reduction of (OEP)In(C_6H_5) and (OEP)In(C_6F_5) in CH_2Cl_2 and this $\Delta E_{1/2}$ can be compared to a 230 mV shift between the $E_{1/2}$ for reduction of (OEP)Fe(C_6H_5) and (OEP)Fe(C_6F_5) under the same experimental conditions (see Figure 6b). Again, the difference in behavior between the two series of compounds is attributed to a difference in the site of electron transfer, i.e., formation of a porphyrin π radical, $[(OEP^{\bullet})M^{III}(R)]^-$, for the main group derivatives and a metal-reduced complex, $[(OEP)Fe^{II}(R)]^-$, for the iron complexes.

Conclusion

This study presents the first overall mechanism to explain the migration reactions of oxidized σ-bonded iron porphyrins which have been identified as intermediates in several biological processes. The data in this paper clearly demonstrate that neither the iron(III) spin state nor the ligand field strength of the σ-bonded axial ligand are in themselves key factors in the occurrence of this reaction. It is shown that all of the investigated compounds undergo three oxidations independent of the axial ligand and that all compounds are oxidized to an Fe(IV) state in the first one-electron transfer step. The first kinetic measurements for rate constants involving the conversion of the singly oxidized species, $[(OEP]Fe(R)]^+$ or $[(OEP)Fe(R)(py)]^+$ to $[(N\text{-ROEP})Fe]^+$, definitively show that the donor ability of the R group accelerates the migration rate while an increased electron donation from the pyridine axial ligand decelerates the migration rate. Consequently, it is proposed that the rate determining intramolecular electron transfer from R to the Fe(IV) center of $[(OEP)Fe(R)]^+$ is the first step in the metal-to-nitrogen migration of the singly oxidized compound.

Acknowledgment. The support of the CNRS and the Robert A. Welch Foundation (K.M.K., E-680) is gratefully acknowledged.

Supporting Information Available: Three figures showing the UV−visible spectra (CH_2Cl_2, 0.2 M TBAP) of low-spin (OEP)Fe(3,4,5-$C_6F_3H_2$), high-spin (OEP)Fe(2,4,6-$C_6F_3H_2$), and $[(OEP)Fe(R)]^+$ complexes and the changes in absorbance bands at $\lambda = 531$ nm due to the loss of $[(OEP)Fe(3,4,5\text{-}C_6F_3H_2)]^+$ and $\lambda = 586$ nm due to the formation of $[(N\text{-}3,4,5\text{-}C_6F_3H_2OEP)Fe]^+$ after the one-electron oxidation of (OEP)-Fe(3,4,5-$C_6F_3H_2$) (1.0×10^{-4} M) by DDQ in deaerated CH_2Cl_2 containing 0.2 M TBAP at 298 K (4 pages). Ordering information is given on any current masthead page.

IC9714706